Preliminary Study on Time-Spectral and Adjoint-Based Design Optimization of Helicopter Rotors

Seongim Choi *
Department of Aeronautics and Astronautics
Stanford University, Stanford, CA 94305

Ki H. Lee †
Aerospace Operations Modeling Branch
NASA Ames Research Center
Moffett field, CA 94035

Juan J. Alonso ‡
Department of Aeronautics and Astronautics
Stanford University, Stanford, CA 94305

Anubhav Datta §
Eloret Corporation
Moffett field, CA 94035

We propose in this paper an adjoint-based design optimization methodology that is particularly efficient for flow simulation of helicopter rotors in combination with a Time-Spectral (TS) method. The TS method is a fast and efficient algorithm to simulate the unsteady periodic flows with the narrow frequency spectrum which are often encountered in rotorcraft, turbomachinery, and fixed-wing flutter analysis. It represents the time discretization of the flow solver by Fourier-based modes/bases in which periodic steady-state is assumed throughout the computation. The steady-state assumption reduces the computational cost significantly, which makes it possible to use the efficient adjoint method applicable to the rotor design problem. The adjoint solution method is widely accepted as an inexpensive way to obtain the sensitivity information of flow solutions to a large number of design parameters. Integrated with gradient-based optimization technique, the adjoint method has been an essential module in aerodynamic/aero-structural shape optimizations. As a preliminary study before we progress towards a more complete and practical desgin optimization of helicopter rotor, this study focuses on the accuracy and validity of our current design optmization tools. First of all, for the validation of the aerodynamic tools, a flight 8534 test condition of the UH-60A configuration is simulated with time-spectral computation, and the accuracy and efficieny of the time-spectral method is demonstrated in comparison with the time accurate results and experimental data. A loose coupling of the time-spectral method and the structural analysis via UMARC is also demonstrated to prove the capability of the time-spectral method to simulate the helicopter rotor problem in a comprehensive way. Finally, a simple design application problem of the hover flight condition is considered and an analysis with single blade coupled with free wake model is employed. A baseline blade shape is modified to an optimal shape to minimize torque while the thrust is maintained or enhanced.

INTRODUCTION

Adjoint method[1,2] has been successfully employed as efficient and accurate technique in a wide range of aerodynamic/aero-structural shape optimization.[3–5] The ability to leverage an adjoint solution to inexpensively obtain the sensitivity of a particular cost function of interest with respect to a large number of design variables has motivated the use of this tool in a variety of design applications. This method becomes critical in the gradient-based optimization process, since the number of design variables can be rather independent of the computational cost, and it provides higher accuracy as opposed to a finite-differencing or complex variable method at a much reduced cost.[3] Therefore a design problem, such as helicopter blade/planform shape optimization, which inevitably involves a large scale simulation with a huge number of design parameters can greatly benefit from the adjoint method.

*Research Associate
†Aerospace Engineer
‡Associate Professor
§Rotorcraft Dynamist

Presented at the AHS Specialist's Conference on Aerodynamics, San Francisco, CA, January 23-25, 2008.

However, until now the application of the adjoint method has been focused mainly on steady-state problems. Unsteady adjoint formulations require storing the entire time history of the flow solutions, which entails massive storage/memory requirements and computational costs.[6] With some efforts[7] to ameliorate this situation, the robustness and efficiency of the truly unsteady adjoint formulation have not yet been fully investigated. Difficulties involved in the implementation of the adjoint formulation for the unsteady flow solvers make the problem more challenging. Therefore because of the difficulties associated with the inherent nature of the complicated unsteady flows around it, its direct application to the design optimization of helicopter rotors has been rather limited and less popular

On the other hand, the Time-Spectral (TS) method[11,14,15] has proved to be very fast and efficient in the simulation of the unsteady periodic flows that often occur in many flight configurations such as pitching airfoils, rotating blades, and flapping wings. A basic idea of the TS method is that a time derivative term in the unsteady flow equation is represented by the inverse Fourier transform of its counterpart in the stationary nonlinear frequency-domain.[8] The pseudo-spectral approach in the frequency domain to simulate the unsteady periodic flows[8] is not specifically new, but the TS method can further contribute to the computational time savings by eliminating the Fourier transformation process back and forth between the time and frequency domain, and also by removing the transient time to reach periodic steady-state. Its accuracy has proved to be equivalent to the conventional time accurate computation.

One of the major advantages of the TS method in our analysis is that it makes the adjoint method applicable to unsteady flow simulations. With the unsteady time response replaced by a Fourier-based representation, the entire computation marches through pseudo-time as it would in a steady-state simulation. Therefore a steady adjoint formulation combined with the TS method becomes amenable to unsteady periodic flows, and any gradient-based optimization method can be easily combined with the adjoint solution method to locate the minimum of the objective function.

Another distinctive characteristic of the flow simulation of helicopter rotors is the significant impacts of the structural loads and deformations on the aerodynamic performance and vice versa. The aerodynamic and structural disciplines are tightly coupled in the helicopter rotor simulation, and the multi-disciplinary aspects of both the flow analysis and the design optimization are inevitable. A number of efforts to couple CFD and computational structural dynamics (CSD) have recently been made with both tight and loose coupling,[17–19] and the results have proved that these approaches are successful. Thus the capability of the TS method to couple with the existing structural/comprehensive analysis tools needs to be investigated so that it can be used with confidence for the analysis and design of helicopter rotors. The cost savings of the TS method should also be able to make the coupling process more efficient.

The main purpose of this study is to examine the accuracy and the validity of our current optimization methodology, which efficiently combines time-spectral and adjoint-based methods, by applying it to real design optimization problems.

A level flight condition of UH-60A configuration, flight 8534, is validated using the time-spectral computation. Flight conditions are simulated using both the time-spectral and time accurate methods, and the results are compared with the experimental data. The time savings using the TS method is shown by directly comparing the wall clock CPU time for both computations.

The validation of the accuracy of time-spectral and discrete adjoint solution method is carried out by simulating the pitching motion of NACA 0012 airfoil. Two flight conditions, supersonic and transonic, are simulated, and the gradients of the average drag coefficient with respect to the local shape changes on the airfoil surface are calculated and compared with finite difference results.

Finally, our design optimization method is applied to a helicopter rotor design problem. Although our methodology has the potential to handle complicated design problems, and the TS method shows great efficiency in highly unsteady problems, we have conducted a preliminary study before moving on to a complete rotor design at the forward flight conditions. A straightforward hover flight condition of the UH-60A configuration is chosen for a test optimization case. Although a hover flight is a steady state, it is treated as periodic unsteady to test our method. To further simplify the problem, a single blade rotor is considered, and a free wake model is added to the computation to include the wake effects. The optimum blade shape to minimize torque at a constant or improved thrust is sought. The shape modifications are imposed by applying Hicks-Henne bump functions with different amplitudes around the airfoil surface at the various sections along the span. Sensitivity information with respect to the shape changes are calculated by the adjoint solution method, and a gradient-based optimization algorithm, a nonlinear multi-dimensional conjugate gradient method in our study, is employed to locate the optimum shape of the blade through the design iterations until the specified convergence is satisfied.

This paper is organized as follows. The details of the time-spectral method and the discrete adjoint solution method are described first, and the validation study is

shown by the simulation of various flow conditions. Finally, results of the blade shape optimization are presented and followed by the conclusion and future work.

TIME-SPECTRAL METHOD

A simulation of helicopter flight inevitably entails the complete computation of three-dimensional rotor. The corresponding computational cost grows rapidly in addition to the complexity related to the mesh construction. Therefore, the efficiency and accuracy of the numerical scheme of the URANS solver becomes crucial. As the flows involved show an unsteady periodic nature, a second order implicit Backward Difference Formula (BDF) has been successfully used for its merit of A-stability, allowing larger time steps than those achieved using an explicit time-stepping method. A set of nonlinear equations for the new state are solved and advanced in time, utilizing inner iterations involving dual time-stepping. Combined with several convergence acceleration techniques,[10] including multigrid and implicit residual smoothing, its efficiency can be remarkably improved. However, the computational cost of this methodology can still be considerably large when applied to unsteady periodic simulations where at least two or three cycles (five or more for a pitching motion) should be preceded before it reaches periodic steady state.

Fully taking the advantage of the periodic nature of the flow, and based on the idea of the Fourier series form of the periodic responses, Hall et.al.[11] proposed Harmonic balance techniques to transform the unsteady equations in the physical domain into a steady problem in the frequency domain. This approach has been extended as a non-linear frequency-domain (NLFD) method[11,12] to Euler and full Navier-Stokes equations and applied to a number of unsteady flow analyses[12] and aerodynamic/aero-structural shape optimization.[8] Compared to the time accurate computations, the NLFD method can achieve a higher efficiency by eliminating the cost to compute initial transient computation to reach the periodic steady-state. However, the solutions we are interested in are in the physical time domain, and thus an inverse Fourier transform back into the time domain is required at each solution iteration, making the frequency-domain method less attractive.

On the other hand, in the same context of the NLFD method of Fourier representations in time, the time-spectral method has been proposed[14] to further improve the efficiency. The main advantage of the TS approach over the frequency-domain method is that the TS method represents the time derivative term in the Navier-Stokes equations as Fourier series directly in the time domain, and therefore eliminates the process required by the frequency-domain method, to in which the solutions must be transformed back and forth to the time domain. The algorithm of the TS method is also more straightforward to implement in RANS solver. Details of the mathematical formulation and stability analysis are described in Reference,[14] and only a brief summary is shown here.

The Navier-Stokes equations in a semi-discrete form in the Cartesian coordinates can be written as

$$V\frac{\partial \omega}{\partial t} + R(\omega) = 0 \ , \tag{1}$$

where ω is the vector of conservative variables,

$$\omega = \begin{pmatrix} \rho \\ \rho u \\ \rho v \\ \rho w \\ \rho E \end{pmatrix} \ , \tag{2}$$

and $R(\omega)$ is the residual of spatial discretizations of viscous, inviscid, and numerical dissipation fluxes.

A discretization of Equation 1 using a pseudo-spectral formula[13] renders equations

$$V D_t \omega^n + R(\omega^n) = 0 \ (n = 0, 1, 2, ..., N-1) \ , \tag{3}$$

where N is the number of time intervals, and D_t is the spectral time derivative operator. If a pseudo-time derivative term is directly added for a time integration to steady state, then Equation 3 becomes,

$$V\frac{\partial \omega^n}{\partial \tau} + V D_t \omega^n + R(\omega^n) = 0 \ (n = 0, 1, 2, ..., N-1) \ . \tag{4}$$

The efficiency of the TS method arises from the treatment of the $D_t\omega^n$ term in Equation 4. Instead of transforming the entire equations into the frequency domain, the inverse Fourier transform is performed only to the time derivative term in Equation 3 as follows,

$$D_t \omega^n = \frac{2\pi}{T} \sum_{k=-\frac{N-1}{2}}^{k=\frac{N-1}{2}} ik\hat{\omega}_k e^{ikn\Delta t} \ (n = 0, 1, 2, ..., N-1), \tag{5}$$

where time period T is divided into N time intervals, $\Delta t = \frac{T}{N}$, and $\hat{\omega_k}$ is a Fourier mode. This can be rewritten in the time domain as suggested,[13]

$$D_t \omega^n = \frac{2\pi}{T} \sum_{m=-\frac{N-1}{2}}^{\frac{N-1}{2}} d_m \omega^{n+m} \ (n = 0, 1, 2, ..., N-1), \tag{6}$$

A term d_m can be rearranged as

$$d_m = \begin{cases} \frac{1}{2}(-1)^{m+1} cosec(\frac{\pi m}{N}) & : m \neq 0 \\ 0 & : m = 0 \ . \end{cases} \tag{7}$$

Thus a time derivative term in Equation 4 behaves as a matrix operator, and an additional cost in the TS method comes from the operation related to the multiplication of the matrix with the elements d_m and the vector ω^{n+m} in Equation 7. The summation in Equation 6 involves the solutions at all time levels, and the solution at each time instance depends upon the solutions at all other time instances. Thus the solution at each time instance is updated simultaneously as the computation advances in the physical time domain until the desired convergence is achieved. This does increase the memory requirement of the TS method, as solutions at all time levels need to be stored. However, if the frequency contents of the problem we are simulating do not span a wide range of the spectrum, this method can considerably contribute to improving the efficiency at an accuracy equivalent to that of the time accurate computations.

DISCRETE ADJOINT METHOD

A design problem in our study can be posed as a general form of the optimization problem which amounts to finding the minimum of the objective/cost function, I, with respect to a number of design variables, x, while satisfying a set of constraints, C. A cost function, I, is also dependent upon the state vector, ω, which can be obtained by solving the governing equations, R. This design problem can be written in mathematical formulation as follows,

$$\begin{aligned} \text{Minimize} \quad & I(x, \omega(x)) \\ \text{w.r.t} \quad & x \ , \\ \text{subject to} \quad & R^*(x, \omega(x)) = 0 \\ & C_i(x, \omega(x)) = 0 \ (i = 1, ..., m) \ , \end{aligned}$$

where the governing equation R^* in our problem represents the time-spectral form of the Euler or Navier-Stokes equations in Equation 4, and m additional constraints are satisfied by the equations $C_i(x, \omega(x))$. The sensitivities of the cost function with respect to the design variables are obtained by applying the chain rule, and a variation of I can be represented, to the first order, as

$$\delta I = \frac{\partial I^T}{\partial \omega}\delta\omega + \frac{\partial I^T}{\partial x}\delta x \tag{8}$$

Since the derivative of the cost function is dependent on both the design variables, x, and the state vector, ω, a new flow solution is required for each parameter with respect to which we are seeking a derivative. As an alternative to the direct solution of Equation 8, we introduce the governing equations as a constraint using the method of Lagrange Multipliers, ψ, which makes it possible to obtain an expression for δI that is independent of $\delta\omega$. The gradient of I with respect to n arbitrary number of design parameters can be calculated without re-evaluating the flow.

In other words, since the governing equations of time-spectral formulation of the Euler/Navier-Stokes equations are given by $R^*(x, /omega) = 0$, we can infer from the fact that the governing equations should always be satisfied, that the variation of the residual must be zero and can be derived as,

$$\delta R^* = \left[\frac{\partial R^*}{\partial \omega}\right]\delta\omega + \left[\frac{\partial R^*}{\partial x}\right]\delta x = 0 \tag{9}$$

As δR^* is identically zero, it can be added or subtracted to Equation 8 to yield,

$$\begin{aligned} \delta I &= \frac{\partial I^T}{\partial \omega}\delta\omega + \frac{\partial I^T}{\partial x}\delta x \ - \\ &\quad \psi^T\left(\left[\frac{\partial R^*}{\partial \omega}\right]\delta\omega + \left[\frac{\partial R^*}{\partial x}\right]\delta x\right) \\ &= \left\{\frac{\partial I^T}{\partial \omega} - \psi^T\left[\frac{\partial R^*}{\partial \omega}\right]\right\}\delta\omega \ + \\ &\quad \left\{\frac{\partial I^T}{\partial x} - \psi^T\left[\frac{\partial R^T}{\partial x}\right]\right\}\delta x \end{aligned} \tag{10}$$

To get rid of the dependence of δI on $\delta\omega$, adjoint variable, ψ can be chosen for the first part of the right hand side of the Equation 10 to be zero. Thus as long as ψ satisfies the adjoint equation,

$$\left[\frac{\partial R^*}{\partial \omega}\right]^T \psi = \frac{\partial I}{\partial \omega} \ , \tag{11}$$

then the sensitivity Equation 8 becomes independent of $\delta\omega$ as follows,

$$\delta I = \left\{\frac{\partial I^T}{\partial x} - \psi^T\left[\frac{\partial R^*}{\partial x}\right]\right\}\delta x \tag{12}$$

The adjoint matrix $\left[\frac{\partial R^*}{\partial \omega}\right]$ in Equation 11 is a sparse matrix of constant coefficients (which depend on the periodic flow solution ω) and can be set up by deriving or computing the dependence of the residual in one cell of the mesh on the flow solution at every cell in the domain. Since the residual evaluation has a compact stencil (mostly composed of nearest neighbors) the number of non-zero entries in each column of the matrix is small. For the current flow solver, SUmb, and the discretization used in this work, the residual at one point is influenced by the flow solution at 33 neighboring cells in Navier-Stokes solutions and 9 cells in Euler solutions. In addition, through the coupling of the time-spectral derivative term, the solution at a point also depends on the solution at the same point, but at all the time instances considered in the solution of the periodic problem. The influence of all other time instances on one is included in an adjoint matrix in a fully coupled manner rather than separated in the right-hand side of the adjoint equation

The computation of all non-zero entries of the matrix and storage during the iterative convergence process requires a considerable amount of memory. Instead, we recompute these terms at every iteration of the adjoint solution, reducing the memory penalty. Furthermore, we have chosen a solution procedure that employs an ILU-preconditioned GMRES algorithm (in the form of the PETSc toolkit) that has proved to be both efficient and robust in the solution of the relatively small problems treated in this work. For larger problems, the convergence rates of this solution approach deteriorate, but the additional multigrid as a preconditioner for the GMRES iteration is able to restore the convergence rates to more reasonable values.

The final sensitivity information in Equation 12 becomes very straightforward to obtain, as $\frac{\partial I}{\partial x}$ and $\frac{\partial R^*}{\partial x}$ are easy to compute. Once we know the objective function values and the gradient information with respect to the design variables, any gradient-based optimization algorithm can be applied to locate the optimum value of the objective function. A conjugate gradient method was chosen in our study. The summary of the entire design optimization procedure is shown at Figure 1.

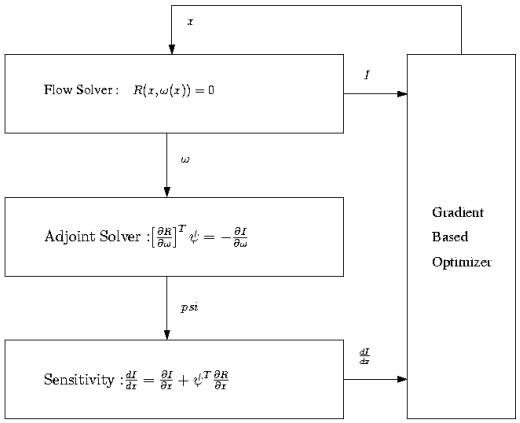

Fig. 1 Procedure for design optimization

VALIDATION OF AERODYNAMIC ANALYSIS TOOL

The accuracy of the analysis tools is crucial to determine the credibility of the design optimization results, and a validation study was performed using our current analysis tools, the time-spectral and adjoint solution method. Simulations of several level flight conditions of a UH-60A configuration were carried out using both the time-spectral and time accurate computation, and the results were compared with experiments. A loose coupling of time-spectral computation with a comprehensive analysis code was also carried out to prove its efficiency for an aerodynamic and structural coupling process.

An adjoint solution method implemented in the time-spectral form of an inviscid flow solver was used to simulate the pitching motion of the NACA 0012 airfoil, and the gradients of a time-averaged drag coefficient with respect to the airfoil shape changes were compared with the finite difference results. An expensive computational cost of the finite difference method has limited the choice of the validation problem to the simple NACA 0012 airfoil, but the accuracy of the current discrete adjoint solution method has been shown to be independent of the size of the problem.

Validation of the Time-Spectral Method

Time-Spectral Computation with Loose Coupling of CFD/CSD

Time-Spectral analysis is coupled to a rotorcraft comprehensive analysis, UMARC (University of Maryland Advanced Rotorcraft Code).[20] The temporal coupling method is unique to rotorcraft and is referred to as 'delta coupling'. The terminology 'loose coupling' is also used by rotary wing researchers to describe this method. However, note that the method bears no resemblance to 'loose coupling' as used by fixed wing researchers. Unlike the 'loose coupling' of fixed wing research, the 'delta coupling' ensures strict time accuracy of the response harmonics. The original 'delta coupling', or 'loose coupling' was proposed by Tung et al.[21] in 1986. In its present form, it has served as the cornerstone of the recent advances in trimmed rotorcraft CFD/CSD loads prediction in the U.S.[17,22,23] and Europe.[24–26] The original method is described in Reference,[21] and its current adaptations in any of the above references (see for example References.[17,22]) For a comprehensive review of the contemporary rotary wing CFD/CSD efforts, see Datta et al.[27]

During the Time-Spectral computation/Comprehensive analysis coupling, the latter supplies the structural dynamic model, the trim model, and the airload sensitivities as required by the delta coupling method. The trim model is a validated full aircraft, six-axes, free flight trim model.[20,22] In the present study, the time-spectral computation is used in its single-blade form. Only the near-field is calculated by RANS. The far-field, which includes the effect of all blades, is accounted for via the inflow generated by a free wake model. The inflow is incorporated within the near-blade CFD domain using the field velocity approach of Sitaraman and Baeder.[28] The wake model is coupled iteratively along with the vehicle trim iterations.

The UH-60A counter 8534 is a vibration critical high speed (155 kts) flight. It is characterized by a speed ratio of $\mu = 0.368$ and the vehicle weight coefficient to solidity ratio $C_W/\sigma = 0.0783$. The calculated thrust coefficient to solidity ratio is $C_T/\sigma = 0.084$. The primary mechanisms of rotor vibratory loads at this flight were identified by Datta and Chopra[29] as: (1) large elastic twist deformations near the blade tip, and (2) inboard wake interactions on the advancing side. The

elastic twist deformations are caused by 3-D unsteady transonic pitching moments near the blade tip, which can only be predicted using CFD. The inboard wake interactions can only be predicted in presence of the correct elastic twist deformations. In the case of single-blade CFD, the inboard interactions can be predicted using a dual peak or a moving vortex type roll-up model. In the present simulation, a moving vortex model was used.

The evolution of predicted pitching moments (approximately a quarter-chord) near the blade tip with coupling iterations is shown in Figure 3. Usually, 6 to 8 iterations are necessary for a converged time accurate solution. The present results correspond to the fourth iteration. The peak pitching moments are correctly predicted near the tip (96.5% R). Thus the primary mechanism of the 3-D unsteady transonic shock relief appears to be in place. The unsteady waveform in the first quadrant, however, is not satisfactory, which can be explained by the fact that this high frequency wake integration can not be captured with TS method unless more time instances are used. The discrepancy is more pronounced at the 92% R.

The pitching moments determine the elastic twist deformations. The twist deformations are shown in Figure 2. The waveforms from the baseline UMARC (unsteady lifting-line based analysis) and CFD are compared with that obtained using measured airloads on the UMARC structural model. In absence of measured deformations, the latter, obtained from a validated structural model,[29] provides a reasonable basis for comparison. The elastic twist deformation shows the same trends as the pitching moments. The general trend is improved (i.e, closer to that obtained using measured airloads). However, the waveform in the first quadrant (between 0 and 90°) shows a significant discrepancy. Capturing the waveform here is important for the accurate prediction of the vibratory lift harmonics (3-20/rev). Even though not accurate, the twist deformation is adequate enough to provide the correct vibratory lift phase near the tip (see Figure 5.) The result of the correct vibratory lift phase is seen in Figure 4, where the phase of the predicted advancing blade lift moves closer, gradually, to that of the test data.

Comparison with Time Accurate Computation

A time-spectral computation has been used to simulate three level flight conditions of the UH-60A configuration as a test cases, flight 8534, 8515, and 9017, and the corresponding sectional force results have been compared with the time accurate results and experiments. Although good agreements for all the test cases have been found and demonstrated in Reference,[16] only the results from the flight 8534 test case are shown in this paper.

Two separate approaches to flow simulation were

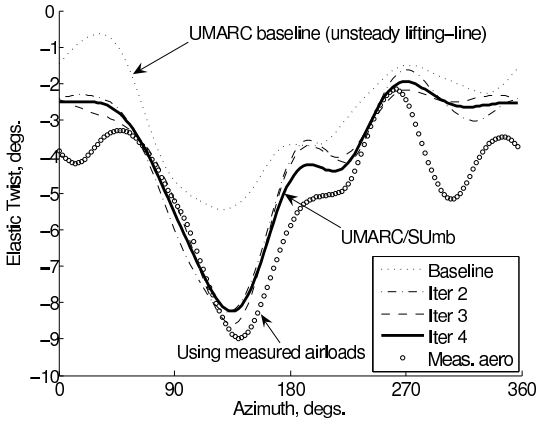

Fig. 2 Changes of twist distribution during coupled runs.

rotating speed (rad/sec)	27.025
M_{tip}	0.6415
M_∞	0.2359
advance ratio	0.368
Reynolds number(chord based)	3.22×10^7
shaft angle (^{o})	-7.31

Table 1 Flight conditions of 8534 test case

considered: single blade analysis with free wake coupling, and complete four blade analysis. A mesh topology for each approach is demonstrated in Figure 6, and the flight condition is summarized at Table 1. A free wake model was added to the single blade analysis to account for the wake effects and other blades. Prescribed deformation obtained from OVERFLOW/CAMRAD analysis was imposed for an aero-elasticity effects, and CFD/CSD coupling is not considered. Time instances of as many as fifteen were used for the time-spectral computation to enhance the accuracy. A previous study[16] indicates that the fewer numbers of time instances were sufficient for the accurate simulation of the flight 8534 case, as the blade and wake interactions were less severe than in the other flight conditions. However the accuracy of the solution appears to be improved for the cases of flight 8515 and 9017 where wake interactions and dynamic stall cycles were not moderate and can not be computed without some higher frequency content.

Figures 17, 18, and 19 show the results of the sectional normal force, chord force, and pitching moment from the single blade analysis. The same flight condition was simulated using four blade analysis and the results are plotted at Figure 20, 21 and 22. Good agreements between single and four blade analysis indicated that the wake interference in flight 8534 was not critical and free wake coupling was a reasonable alternative to the complete wake capturing method at a better computational cost.

A computational time saving for time-spectral computation was estimated by a direct comparison with

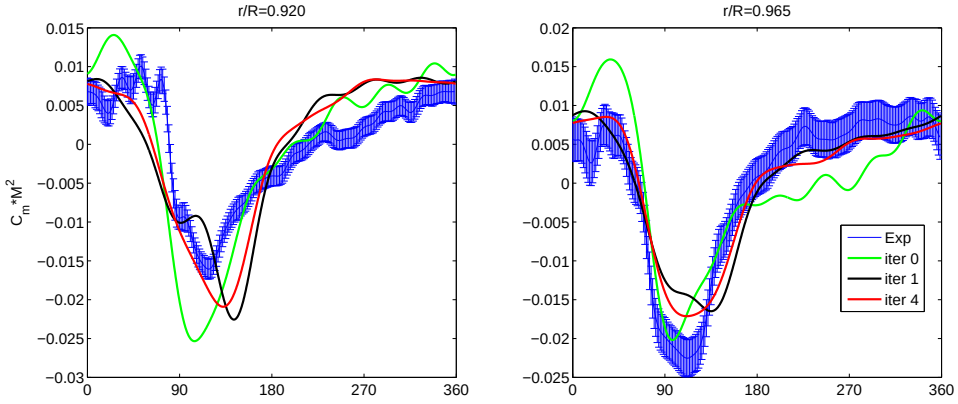

Fig. 3 Changes of sectional pitching moment during coupled runs.

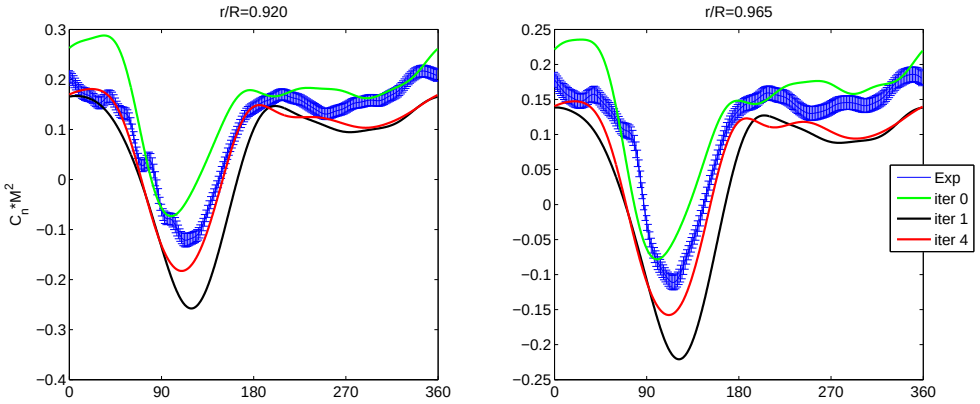

Fig. 4 Changes of sectional normal forces (0/rev∼20/re) during coupled runs.

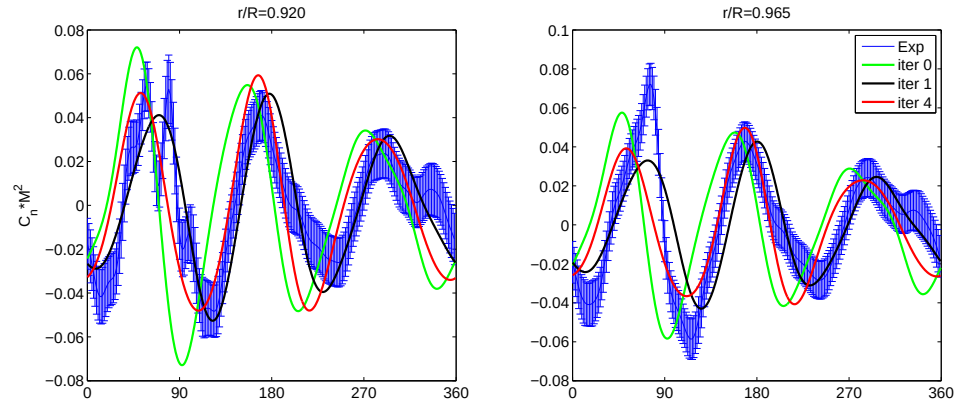

Fig. 5 Changes of sectional normal forces (3/rev∼20/rev) during coupled runs.

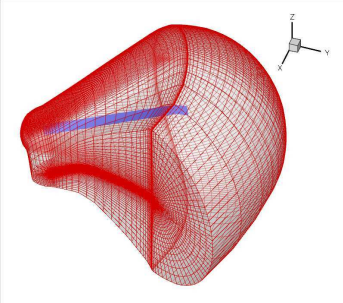

a) C-O-type mesh around single blade (single-block with 568,816 nodes)

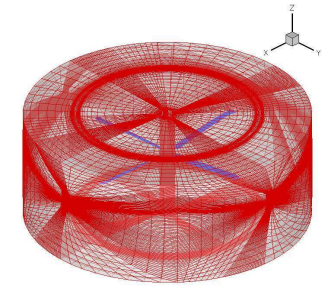

b) mesh around 4 blades (536 blocks with 2,401,776 nodes)

Fig. 6 Grid topology for UH60

computation method	Time (sec) /per one MGcycle
time accurate	4.47
time spectral (9 time instances)	49.611
time spectral (15 time instances)	92

Table 2 Comparison of wall clock CPU time between time-spectral and time accurate method.

a time accurate computation of wall clock CPU time for the flight 8534 simulation using single blade analysis with the results shown in Table 2. Scaling factors of five or more were observed for both computations, to be converged up to 10^{-4} order (from the L2 norm-based residual of the density). A conventional second order BDF scheme was used with a time accurate scheme, 30 multigrid inner iterations, $0.2 \sim 0.3^o$ time step and $2 \sim 3$ revolutions. Nine to fifteen time instances were used in time-spectral computation. We also employed a free wake coupling method for a hover flight simulation, which is considered in the design optimization application. The computational time saving is critical for the optimization procedure to shorten its turnaround time for function evaluations.

Validation of Time-Spectral and Adjoint Solution Method

A good way to validate the accuracy of the proposed methodology is to compare the sensitivity information with other gradient computation methods that have equivalent accuracy. Such methods as finite difference, complex variable and automatic differentiation methods have different characteristics in their accuracy and computational cost. A finite difference method was chosen for the comparison as its implementation is easy and straightforward; however the step sizes are carefully taken to minimize the dependence on the step sizes. On the other hand, the Automatic Differentiation (AD) method[31] uses numerical algorithm to evaluate the adjoint solutions by a computer program. It achieves numerical accuracy higher than that of the manual derivation as it is not associated with round-of errors due to democratization or cancellation errors due to finite number precision. Its application to the solution of discrete adjoint method is currently being pursued.

A pitching motion of a NACA 0012 airfoil was simulated at two flow conditions, both transonic ($M_\infty = 0.8$) and supersonic ($M_\infty = 2.0$) inviscid flows. The airfoils were pitched about the quarter chord with a reduced frequency of $k = 0.2$ and with a pitching motion amplitude of $\pm 5^o$. The corresponding angular frequencies were $\omega = 35.43, 88.5$HZ for the transonic and supersonic flow condition respectively. The test cases presented here are quasi-three-dimensional in that they consist of a two-dimensional airfoil extruded in the third direction. A total of six time instances for a period of the pitching motion were used for both the flow and discrete adjoint solution. A body-fitted O-mesh with $81 \times 17 \times 9$ grid points were used for all the calculations. Figure 7 shows Mach number contours for four snapshots of the time-spectral solution for the transonic test case, and the supersonic case is shown in Figure 8. A comparison of the time-spectral results, with a time accurate computation using second-order backwards difference formula and a dual time-stepping approach, has shown good agreements, although the comparison is not included in this paper. A similar agreement is found for the supersonic flow simulation.

The corresponding snapshots for the discrete, time-spectral, and adjoint solutions for both the transonic and supersonic cases (for the first adjoint variable only) can be found in Figures 9 and 10. To assess the accuracy of the resulting discrete adjoint solution, a finite difference method was used to compare the sensitivity of the time-averaged coefficient of drag

$$\overline{C_D} = \frac{1}{T}\int_0^T C_D(t)dt \tag{13}$$

with respect to the amplitude of Hicks-Henne bump functions centered at mesh points on the upper surface of the airfoil. The Hicks-Henne functions are smooth functions that can be used to modify the shape of the NACA 0012 airfoil. Their effect (appropriately non-dimensionalized) can be seen in Figure 12.

The values of the sensitivities of the average drag coefficient (over a pitching cycle), $\overline{C_D}$ (shown in Fig-

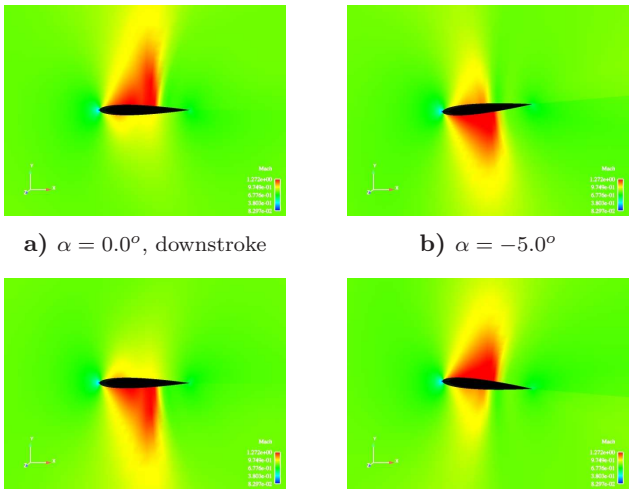

a) $\alpha = 0.0^o$, downstroke **b)** $\alpha = -5.0^o$

c) $\alpha = 0.0^o$, upstroke **d)** $\alpha = 5.0^o$,

Fig. 7 Four snapshots of the local Mach number contours for a pitching NACA 0012 airfoil in transonic flow, $M_\infty = 0.8, k = 0.2, \Delta\alpha = \pm 5^o$

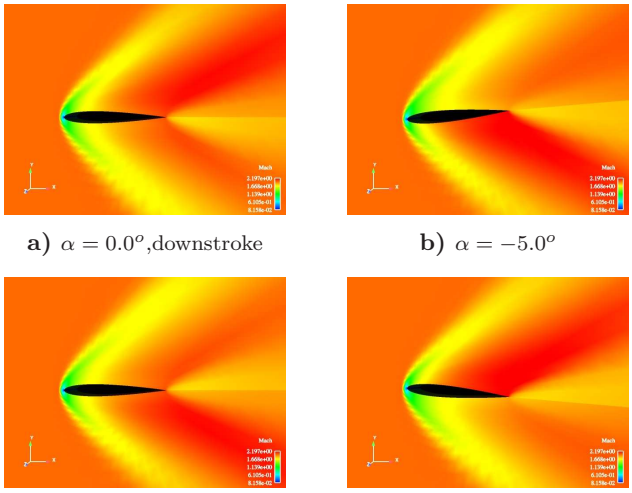

a) $\alpha = 0.0^o$,downstroke **b)** $\alpha = -5.0^o$

c) $\alpha = 0.0^o$,upstroke **d)** $\alpha = 5.0^o$,

Fig. 8 Four snapshots of the local Mach number contours for a pitching NACA 0012 airfoil in supersonic flow, $M_\infty = 2.0, k = 0.2, \Delta\alpha = \pm 5^o$

ure 11) computed using both the time-spectral adjoint solutions and the method of finite differences (with carefully chosen step sizes to yield accurate derivatives). The agreement between these two approaches gives us confidence that the results of the time-spectral adjoint calculations are correct. Small differences between the two sets of results still exist, and are attributed to the fact that the time-spectral adjoint operator we have implemented has neglected some variations of the residual $R^*(w)$ involving the spectral radius computation and the artificial dissipation coefficients.

RESULTS

The main purpose of the current study is to assess the validity and accuracy of the current design

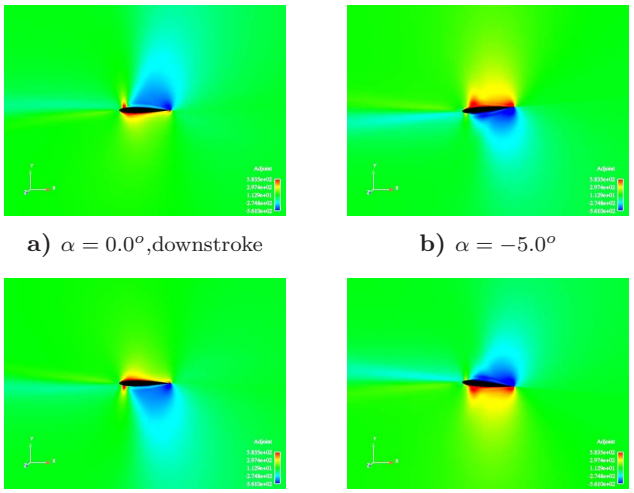

a) $\alpha = 0.0^o$,downstroke **b)** $\alpha = -5.0^o$

c) $\alpha = 0.0^o$,upstroke **d)** $\alpha = 5.0^o$,

Fig. 9 Four snapshots of the local Mach number contours of the first adjoint variable for a pitching NACA 0012 airfoil in transonic flow, $M_\infty = 0.8, k = 0.2, \Delta\alpha = \pm 5^o$

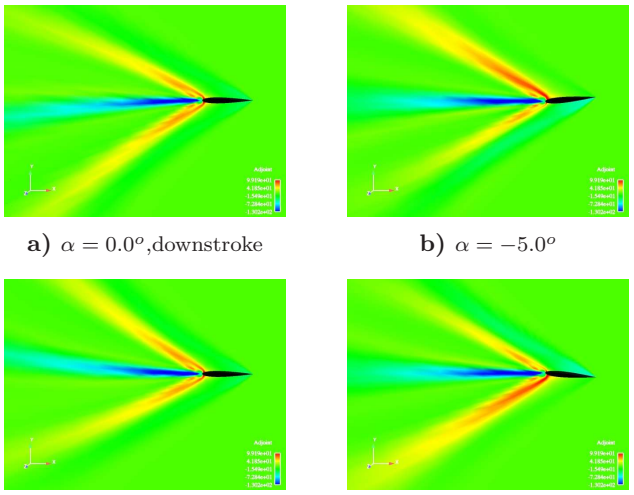

a) $\alpha = 0.0^o$,downstroke **b)** $\alpha = -5.0^o$

c) $\alpha = 0.0^o$,upstroke **d)** $\alpha = 5.0^o$,

Fig. 10 Four snapshots of the local Mach number contours of the first adjoint variable for a pitching NACA 0012 airfoil in supersonic flow, $M_\infty = 2.0, k = 0.2, \Delta\alpha = \pm 5^o$

optimization tool and to investigate its capability for future applications to more viable and complete design problems. A simple yet realistic rotorcraft problem is considered in this paper. The choice of the hover flight condition made the optimization problem more straightforward, as the trim condition was not violated exceedingly. An optimum blade shape that minimized torque was sought while a total thrust produced by the baseline configuration was maintained constant or enhanced. A blade of UH-60A configuration was chosen for the baseline, and single blade analysis described from the earlier section was carried out with the mesh topology shown at Figure 6(a). An M_{tip} was 0.65, and fixed collective pitch angle was set

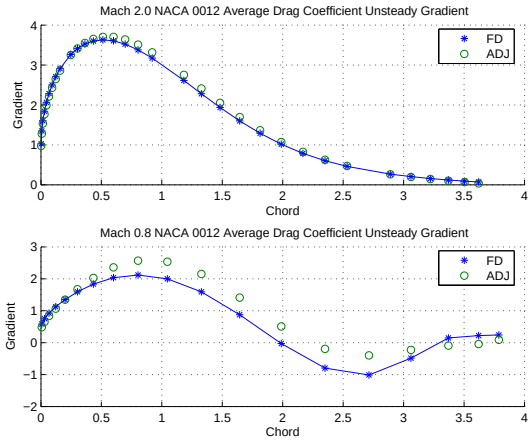

Fig. 11 Comparison of sensitivity derivatives $\frac{\partial C_D}{\partial b_i}$ using discrete adjoint solution and finite differences for the supersonic (top) and transonic (bottom) test cases.

11.8°. A total of three time instances were used for time-spectral computation and the aero-structural deformation was prescribed at each time instance from the previous analysis using OVERFLOW/CAMRAD computation.[17]

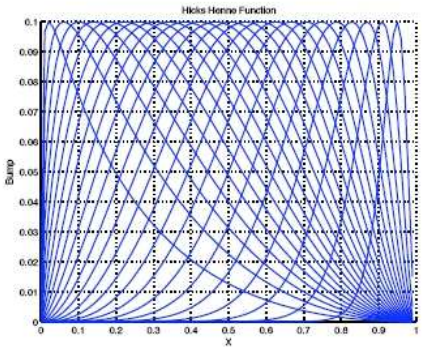

Fig. 12 Non-dimensional effect of Hicks-Henne perturbation on the surface of the airfoil.

Another advantage of optimizing the hover condition is that constraint handling became more straightforward as the number of constraints was reduced by excluding the trim related parameters. We employed a nonlinear multi-dimensional conjugate gradient method for a gradient-based optimization algorithm. Since the constraint handling in conjugate gradient method was not straightforward, a constraint of constant thrust was integrated into the objective function as an implicit form via the properly weighted penalty.Also a second form of an objective function without a constraint of constant thrust was considered as the ratio of torque to thrust, if improved thrust is allowed.

Using the nondimensionalized coefficients of torque and thrust, mathematical formulations of the objective functions are shown at Equation 14,

$$\begin{aligned} I &= C_Q/C_T \ , \\ I &= C_Q + \alpha \left((C_{T_o} - C_T) \right)^2 , \end{aligned} \tag{14}$$

where C_Q and C_T are the coefficient of torque and thrust, respectively, after the blade shape is modified, and C_{T_o} is the coefficient of the initial thrust of the baseline. Blade shape modifications were obtained by imposing smooth Hicks-Henne bump functions on the surface of the airfoils along the various span sections, and the corresponding new meshes were generated using the mesh warping routine without the need for the regenerating the complete meshes. As the gradient-based optimization algorithm performs well with the smooth design space, the shape changes, thus the amplitudes of the bump functions are limited to small amounts, with the assumption that few variations in the shape modifications produces smooth design space and less deviation in structural deformation from the initial values. A total of nine sections along the span were selected, with even distribution on the blade midboard sections and close distribution on the blade inboard sections and tip sweep region. Perturbations were applied at each section on ten locations of the airfoil surfaces, and the maximum amplitudes of the bumps were scaled to the local airfoil thickness. A total of 90 design variables (the amplitudes of bump functions) were introduced, and it has been tested that the inclusion of more design variables do not significantly affect the results.

Prescribed aero-elastic deformation was set as constant, and maintained as the initial value throughout the design iterations where the blade shape changed, although this is not practically true. If the blade shape were to experience significant variation, such as that required for planform shape optimization, structural deformation must be properly updated at each design iteration through CFD/CSD coupling. However, when we introduced a small changes only in design variables, we assumed that aero-elastic deformation would not deviate much from the initial values.

Optimized results were obtained after 19 design iterations and a total of 12% torque reduction at the 7% thrust increase. These values came at a surprise, considering the small variations in the airfoil shapes (mainly camber changes), but this fact implies that aerodynamic loads are very sensitive to even small changes in the airfoil shapes. The corresponding shape of the optimized blade is shown at Figures 13 and 14. As the shape changes are limited to the small variations, the direct comparison of shapes between the baseline and the optimized blade is not obvious.

Changes in the pressure distribution on the blade are demonstrated in Figures 15 and 16 on the upper and lower surfaces respectively. It can be noted that pressure around the tip area becomes lower and contributes to reducing the pressure drag.

CONCLUSIONS AND FUTURE WORK

A new optimization methodology was proposed based on the combined time-spectral and adjoint-based approaches for the design problem involving unsteady periodic flows. The accuracy and efficiency of the time-spectral solution method was validated by the simulation of the flight 8534 test case of the UH-60A configuration, and the results showed good agreements with time accurate results and the experimental data. The adjoint solution method with the time-spectral implementation of the flow solver was applied to the simulation of the pitching motion of a NACA 0012

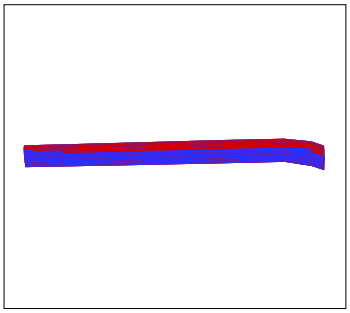

a) overlaid blade shapes (upper surface), red:baseline, optimized:blue

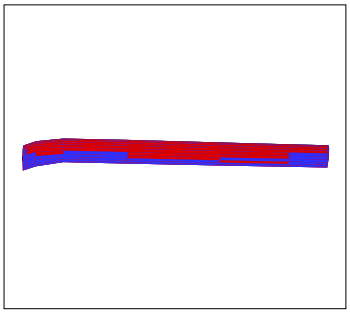

b) overlaid blade shapes (lower surface), red:baseline, optimized:blue

Fig. 13 Comparison of blade shapes between baseline(red) and optimized(blue)

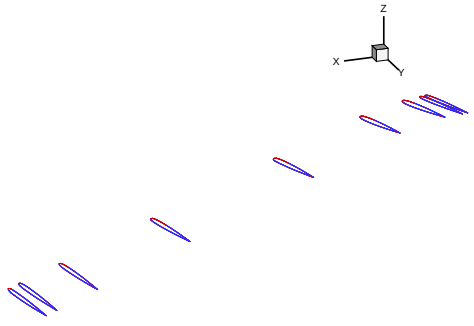

Fig. 14 Shape changes of the airfoils along the span (baseline(red) and optimized(blue)).

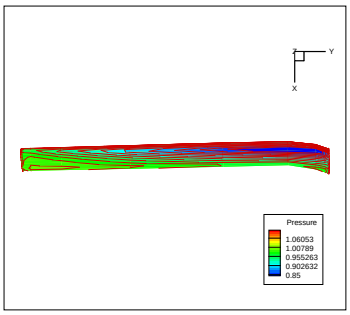

a) baseline

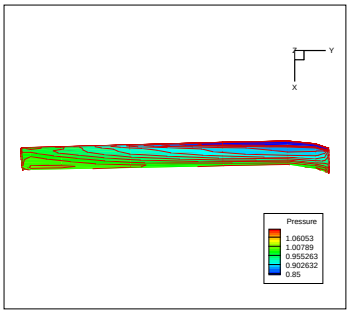

b) optimized

Fig. 15 Comparison of the surface pressure contours between the baseline and the optimized (on the upper surface).

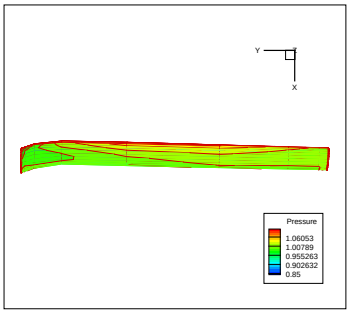

a) baseline

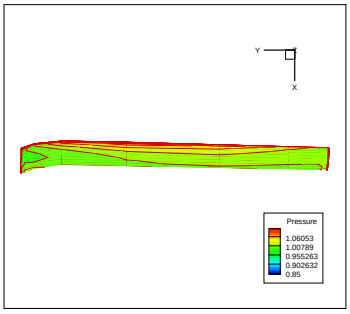

b) optimized

Fig. 16 Comparison of the surface pressure contours between the baseline and the optimized (on the lower surface).

airfoil, and the gradients of the time-averaged drag coefficient with respect to the airfoil shape changes were compared with the finite difference results. Good agreements were found for both the supersonic and transonic flow conditions. Finally a simple optimization problem was solved for a helicopter blade shape design at the hover flight condition. A minimization of torque at a constant or improved thrust was pursued by a multi-dimensional conjugate gradient method. As much as 12% reduction of torque was observed, while the total thrust was enhanced by 7%. This fact indicates that our design optimization methodology is suited for helicopter rotor design. However, to fully employ our methodology to realistic design cases of helicopter rotors, such as at the forward flights, a number of issues should be resolved. First, a study on the proper choice of design variables should proceed for a realistic helicopter rotor design. More design variables, in addition to the design variables not only limited to the camber changes in our study, will be able to produce further improvement in aerodynamic performance. However, when adjoint-based optimization uses gradient information to locate optimum values, special care must be taken to ensure smooth design space.

A more viable design test for helicopter flight is to optimize the rotor shapes during the forward flight condition, where our design approach using time-spectral solution method is best suited. However highly unsteady motion during the forward flight poses numerous problems. A more rigorous form of constraints to satisfy the trim condition needs be included in the optimization process, and a more efficient and robust constrained optimization algorithm is necessary. Our design methodology is currently tested with NPSOL SQP method and ready to be applied to the realistic design optimization of helicopter rotors, and optimization results with a better optimization algorithm will be shown in the future. Finally the current adjoint solver implementation in the Euler flow solver will be extended to the full Navier-Stokes flow solver. Introducing an automatic differentiation algorithm[31] would enable the adjoint solver development to be easier and more straightforward, and this is also part of our on-going research.

Acknowledgment

This work has been carried out under the support of the AFDD at Ames Research Center, under contract NNA06CB11G. We gratefully acknowledge the support of our points of contact, Mark Potsdam and Tom Maier, in supplying us with the experimental data necessary to complete this study.

References

[1]J.J.Reuther, A. Jameson, J.J.Alons, M.Rimlinger, and D.Saunders, " Constrained multipoint aerodynamic shape optimization using an adjoint forumlation and parallel computers: Part I & II," *Journal of Aircraft, 36(1):51-74*,1999

[2]A. Jameson, "Aerodynamic design via control theory ," *Journal of Scientific Computing, 3:233-260*,1988

[3]J.R.R.A.Martins, "A Coupled-Adjoint Method for High-Fidelity Aero-Structural Optimization," *ph.D dissertation*, Department of Aeronautics and Astrounautics, Stanford University, Stanford, CA, Oct. 2002.

[4]S. Kim, J.J.Alonso, and A.Jameson, "A gradient accuracy study for the adjoint-based Navier-Stokes design method," *AIAA Paper 99-0299*,Reno, Jan. 1999.

[5]K.Leoviriyakit and A.Jameson, "Aero-structural wing planform optimization," *AIAA 42nd Aerospace Science Meetings & Exhibit,*Reno, NV, Jan. 2004.

[6]K. Mani, D. J. Mavriplis, "An Unsteady Discrete Adjoint Formulation for Two-Dimensional Flow Problems with Deforming Meshes," *AIAA 45th Aerospace Science Meetings & Exhibit,*Reno, NV, Jan. 2007.

[7]K.Palaniappan, P.Sahu, J.J.Alonso, and A.Jameson, "Active flutter control using an adjoint method," *AIAA Paper 2006-0844*, Reno, NV, Jan. 2006.

[8]S.Nadarajah, M.McMullen, and A.Jameson, "Optimal control of unsteady flows using time accurate and non-linear frequency domain methods," *AIAA Paper 2003-3875*,Orlando, FL, Jun. 2003.

[9]S.Nadarajah and A.Jameson, "A comparison of the continuous and discrete adjoint approach to automatic aerodynamic optimization," *AIAA Paper 2000-0677*,Reno, NV, Jan. 2000.

[10]A. Jameson, "Time dependent calculations using multigrid, with application to unsteady flows past airfoils and wings," *AIAA Journal, 91-1956,* June 1998.

[11]J.P.Thomas, E.H.Dowell, and K.C.Hall, "Modeling three-dimensional inviscid transonic limit cycle oscillation using a harmonic balance approach," *ASME International Mechanical Enginnering Conference and Exposition*,New Orleans, 2002.

[12]M. S. McMullen, "The Application of Non-Linear Frequency Domain Methods To the Euler and Navier-Stokes Equations ," *Ph.D thesis, Stanford University,* March 2003.

[13]C. Canuto, M. Y. Hussaini, A. Quarteroni, T. A., Jr. Zang "Spectral Methods in Fluid Dynamics," *Springer,* 1998.

[14]A. Gopinath and A. Jameson, "Time spectral method for periodic unsteady computations over two- and three- dimensional bodies," *AIAA Paper 05-1220*, Reno, NV, Jan. 2005.

[15]E.van der Weide, A.Gopinath and A.Jameson, "Turbomachinery applications with the time spectral method," *AIAA Paper 05-4905*, Toronto, Canada, Jun. 2005.

[16]S. Choi, J. J. Alonso, E. van der Weide, and J. Sitaraman, "Validation Study of Aerodynamic Analysis Tools for Design Optimization of Helicopter Rotors," *AIAA Paper 07-3929*, Miami FL., June 2007.

[17]M.Potsdam, H.Yeo, and W.Johnson, "Rotor Airloads Prediction Using Loose Aerodynamic/Structural Coupling," *AHS 60th Annual Forum*, Baltimore MD, June 7-10 2004.

[18]A. Datta, and I. Chopra, "Prediction of UH-60A Dynamic Stall Loads in High Altitude Level Flight using CFD/CSD Coupling," *AHS 61st Annual Forum*, Grapevine, TX, June 1-3 2005.

[19]M. J. Bhagwat, R. A. Ormiston, H. A. Saberi, and H. Xin, "Application of CFD/CSD Coupling for Analysis of Rotorcraft Airloads and Blade Loads in Maneuvering Flight," *AHS 63rd Annual Forum*, Virginia Beach VA, May 1-3 2007.

[20]Datta, A., Chopra, I., "Validation and Understanding of UH-60A Vibratory Loads in Steady Level Flight," *Journal of the American Helicopter Society*, Vol. 49, No. 3, July 2004, pp 271-287.

[21]Tung, C., Cardonna, F.X., and Johnson, W.R., "The Prediction of Transonic Flows on an Advancing Rotor," *Journal of the American Helicopter Society*, Vol. 31, (3), July 1986, pp. 4–9.

[22]Datta, A., Sitaraman, J., Chopra., I, and Baeder, J., "CFD/CSD prediction of rotor vibratory loads in high speed

flight," in press, *Journal of Aircraft*, Vol. 43, (6), November–December 2006, pp. 1698–1709.

[23]Datta, A. and Chopra, I., "Prediction of UH-60 Main Rotor Structural Loads using CFD/Comprehensive Analysis Coupling," *32nd European Rotorcraft Forum*, Maastricht, The Netherlands, September 12–14, 2006.

[24]Servera, G., Beaumier, P., and Costes, M. "A Weak Coupling Method between the Dynamics Code Host and the 3D Unsteady Euler Code Waves," *26th European Rotorcraft Forum*, The Hague, Netherlands, September 14–16, 2000.

[25]Altmikus, A. R. M., Wagner, S., Beaumier, P., and Servera, G., "A Comparison : Weak versus Strong Modular Coupling for Trimmed Aeroelastic Rotor Simulation," *American Helicopter Society 58th Annual Forum*, Montreal, Quebec, June 2002.

[26]Pahlke, K. and Van Der Wall, B., "Chimera simulations of multibladed rotors in high-speed forward flight with weak fluid-structure-coupling," *Aerospace Science and Technology*, Vol. 9, (5), 2005, pp. 379–389.

[27]Datta, A., Nixon, M. and Chopra, I., "Review of Rotor Loads Prediction with the Emergence of Rotorcraft CFD," *Journal of the American Helicopter Society*, Vol. 52, (4), October 2007, pp. 287–217.

[28]Sitaraman, J. and Baeder, J., "Field Velocity Approach and Geometric Conservation Law for Unsteady Flow Simulations," *AIAA Journal*, Vol. 44, (9), September 2006, pp. 2084–2094.

[29]Datta, A., and Chopra, I, "Validation of Structural and Aerodynamic Modeling using UH-60A Airloads Program Data," *Journal of the American Helicopter Society*, Vol. 51, (1), January 2006, pp. 43–58.

[30]J. W. Lim, T. A. Nygaard, R. Strawn, and M. Potsdam, "Blade-Vortex Interaction Airloads Prediction Using Coupled Computational Fluid and Structural Dynamics," *Journal of the American Helicopter Society*, Vol. 52, (4), October 2007, pp. 43–58.

[31]A. C. Marta, "Rapid Development of Discrete Adjoint Solvers With Applications To Magnetohydrodynamic Flow Control," *Ph.D thesis, Stanford University,* June 2007.

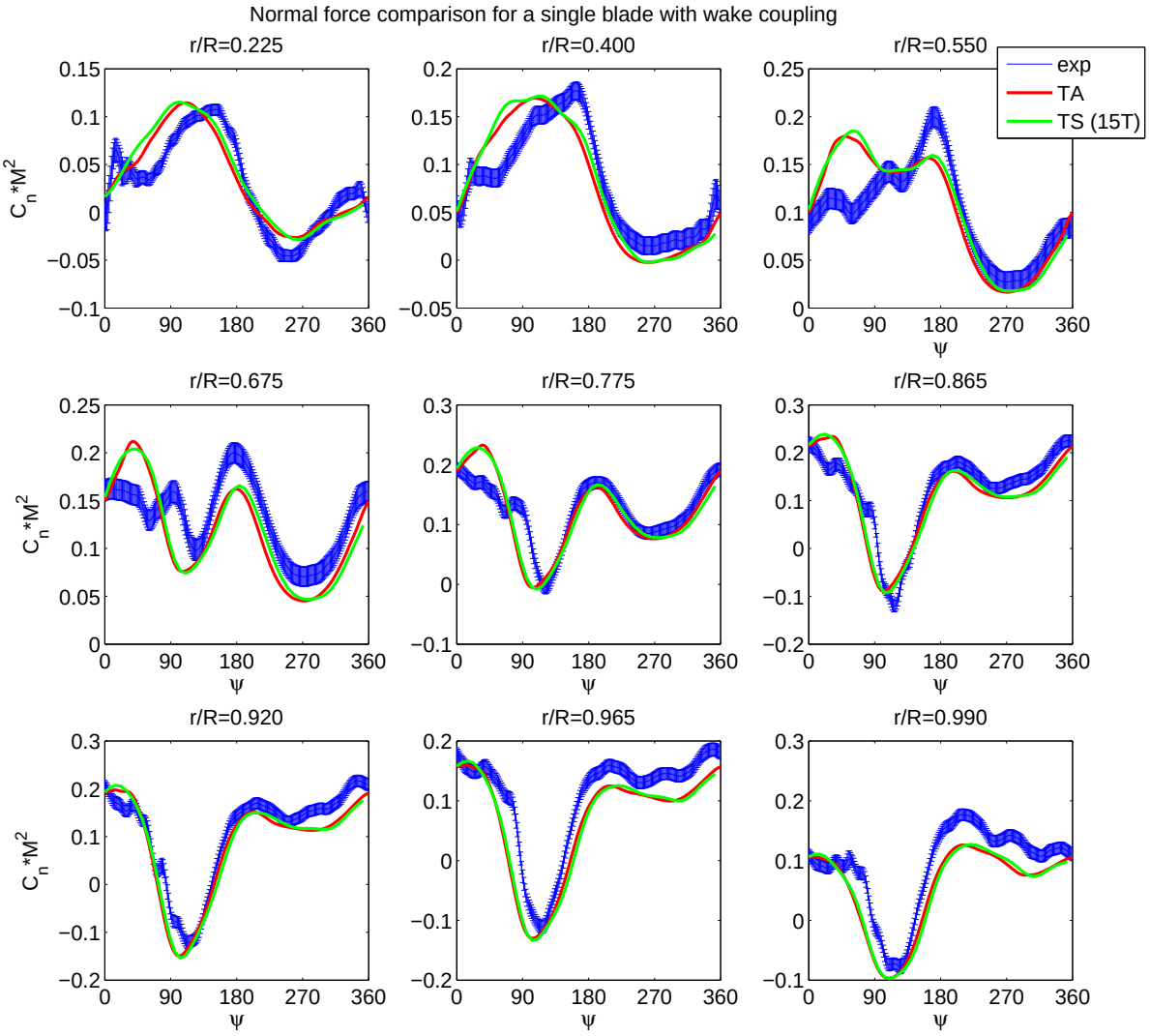

Fig. 17 Section normal force of flight 8534 (one blade case with wake coupling (red-TA; green-TS)).

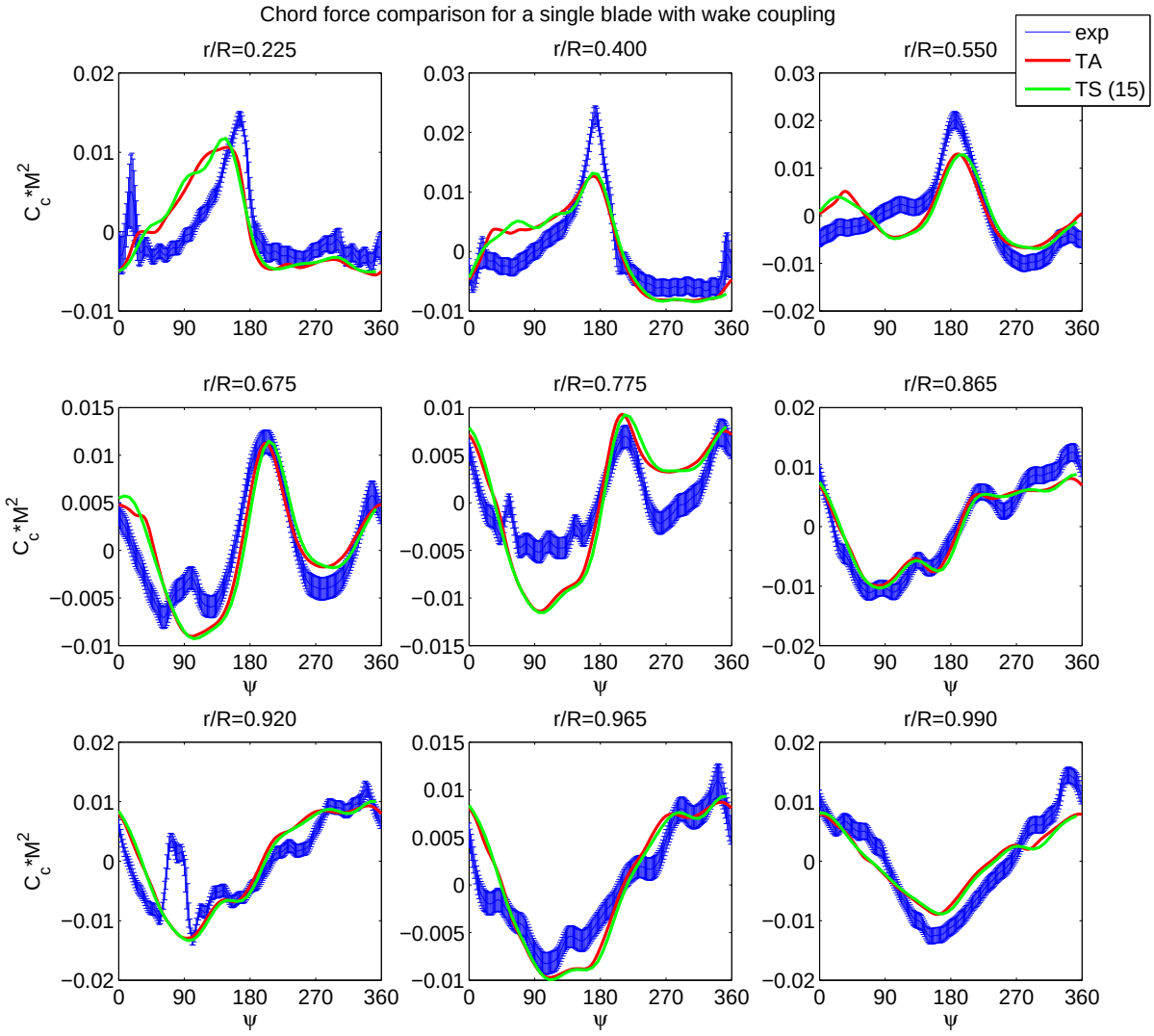

Fig. 18 Section chord force of flight 8534 (one blade case with wake coupling (red-TA; green-TS)).

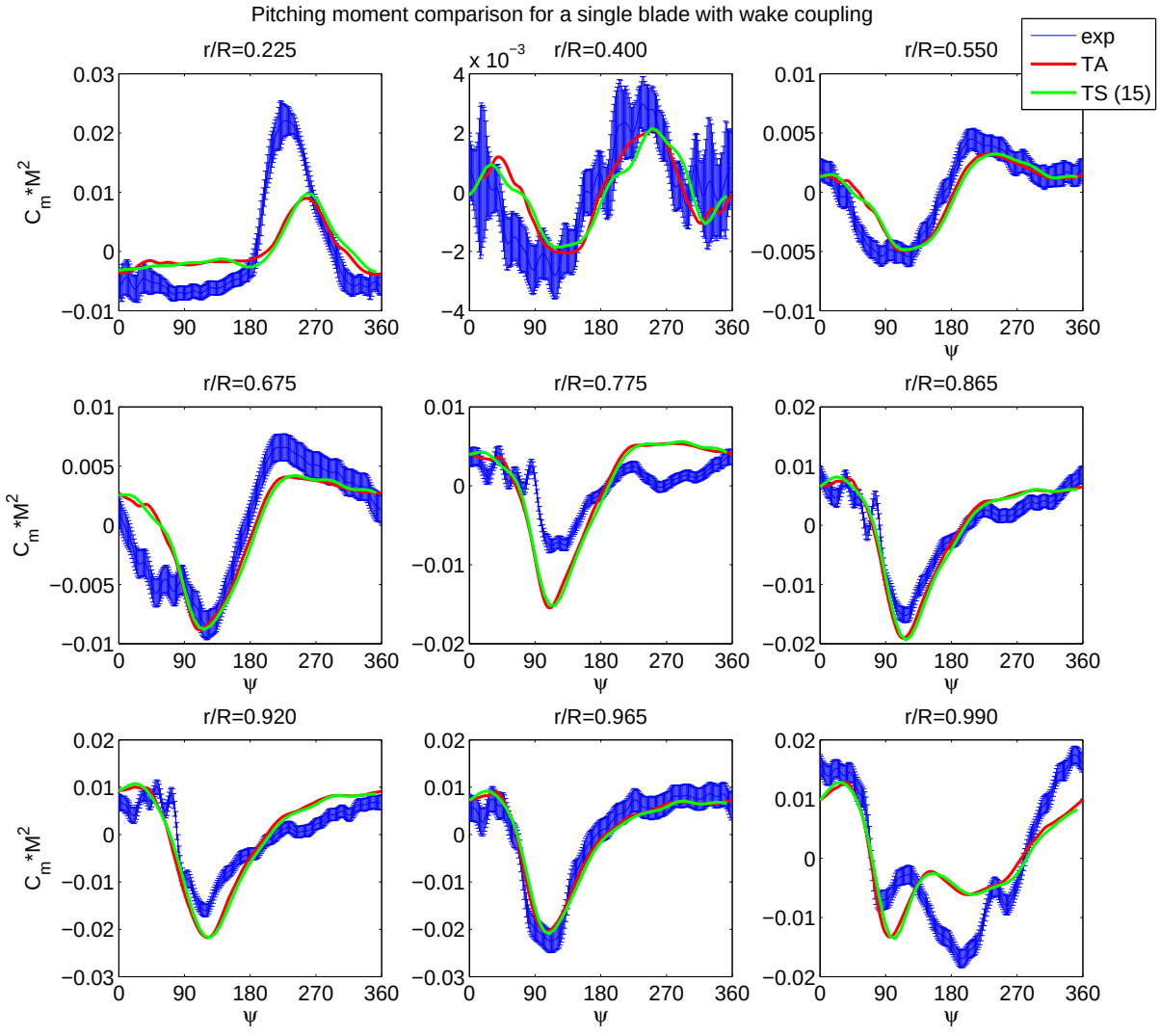

Fig. 19 Section pitching moment of flight 8534 (one blade case with wake coupling (red-TA; green-TS)).

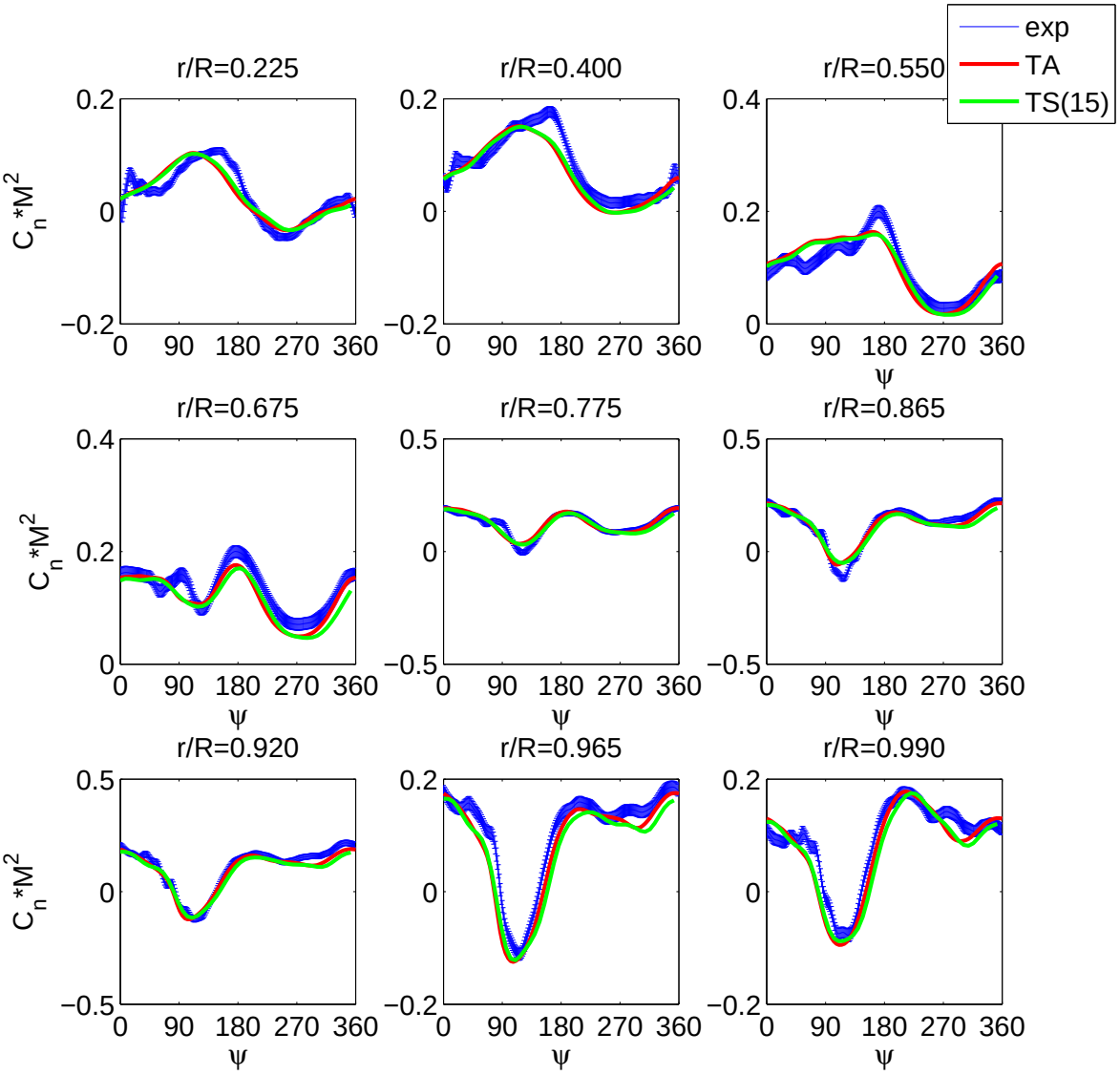

Fig. 20 Section normal force of flight 8534 (four blade case (red-TA; green-TS)).

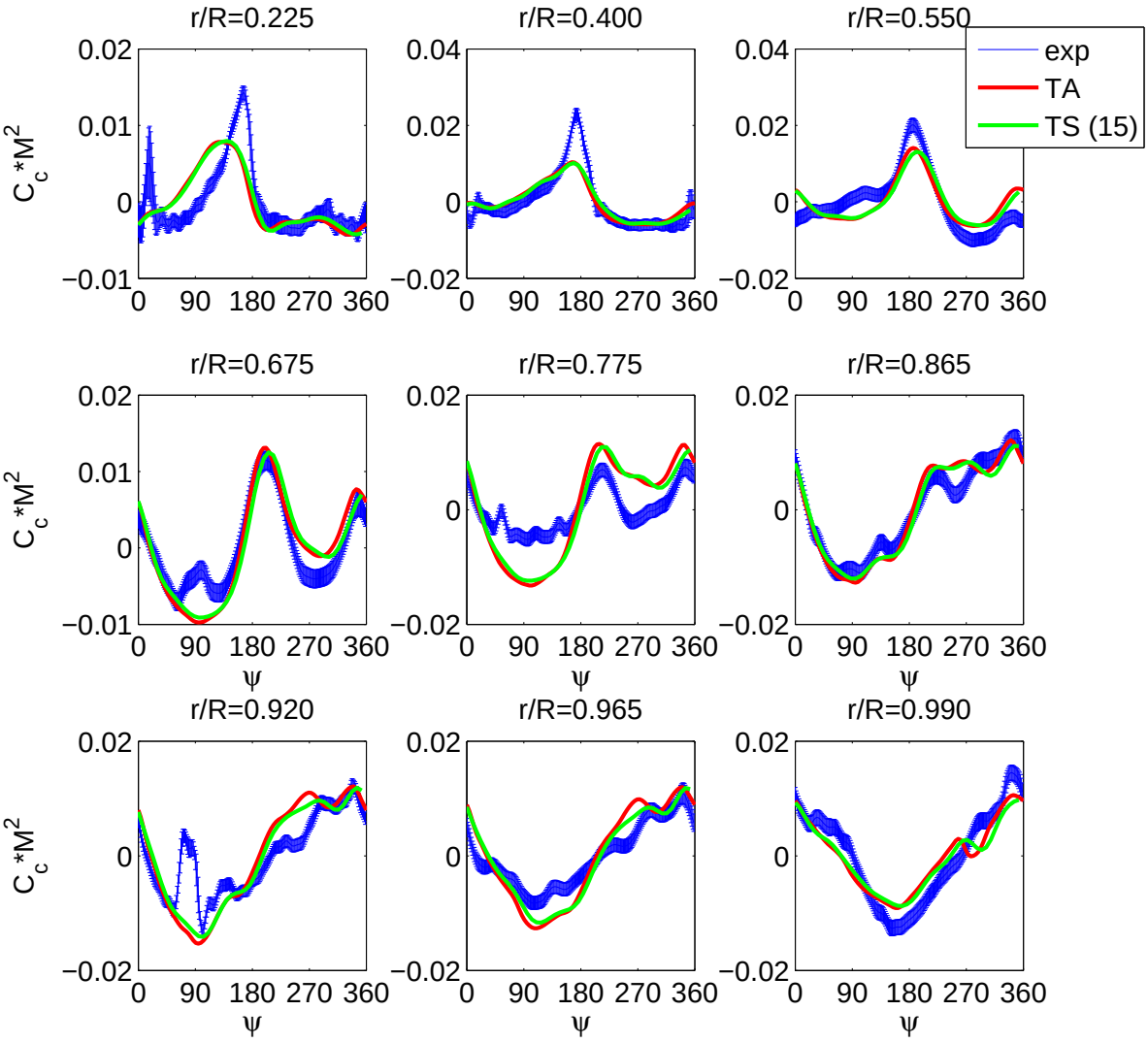

Fig. 21 Section chord force of flight 8534 (four blade case (red-TA; green-TS)).

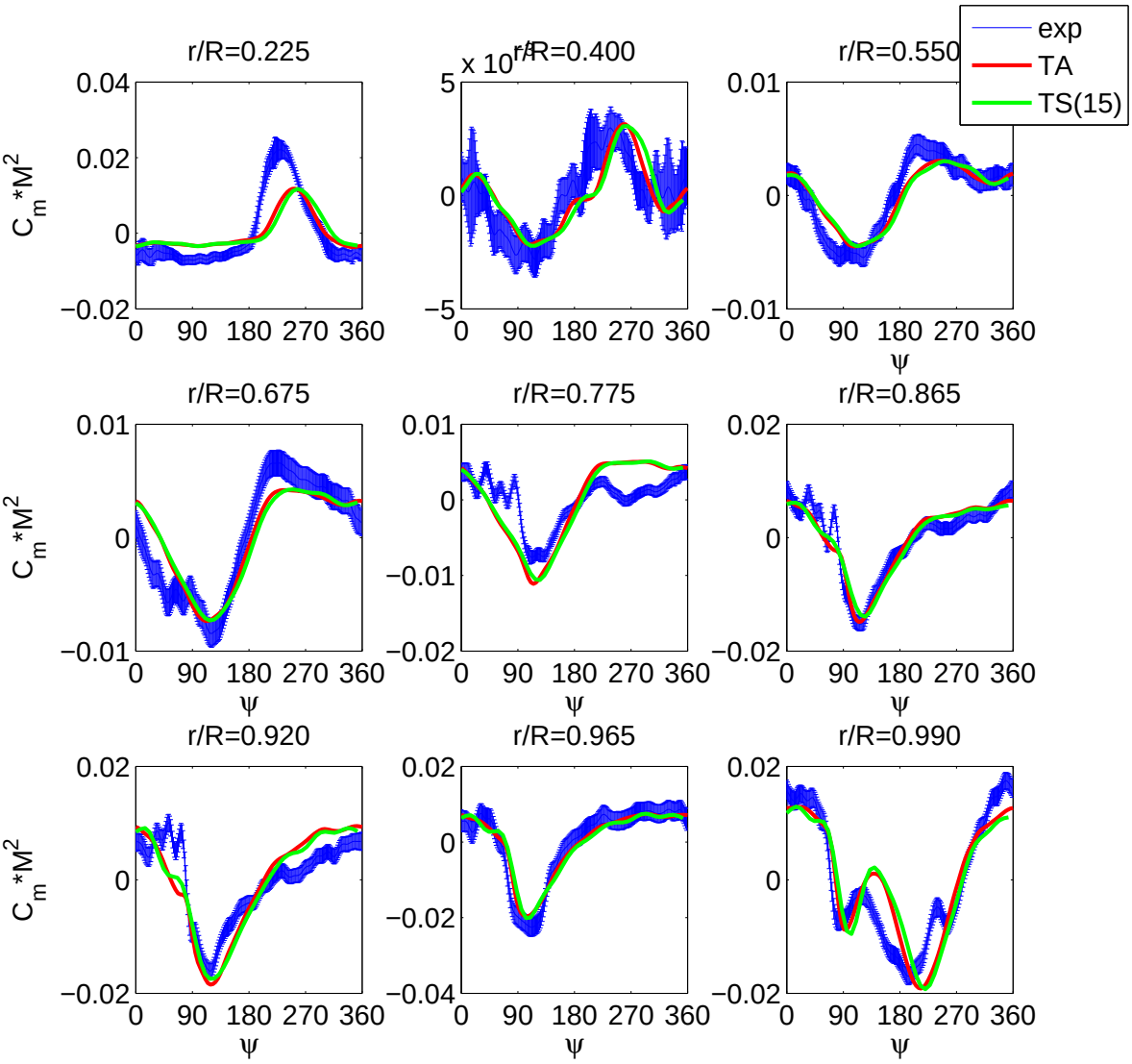

Fig. 22 Section pitching moment of flight 8534 (four blade case (red-TA; green-TS)).